

# AN INVERSE PROBLEM OF TRANSIENT THERMOELASTICITY IN RETRIEVING BOUNDARY CONDITIONS

Masataka TANAKA <sup>1)</sup>, Artur GUZIK <sup>2\*)</sup>, Toshiro MATSUMOTO <sup>3)</sup>

1) Faculty of Engineering, Shinshu University, (Nagano 380-8553, e-mail: dtanaka@gipwc.shinshu-u.ac.jp)

2) Faculty of Engineering, Shinshu University, (Nagano 380-8553, e-mail: guzik@homer.shinshu-u.ac.jp)

3) Faculty of Engineering, Shinshu University, (Nagano 380-8553, e-mail: toshiro@gipwc.shinshu-u.ac.jp)

\* while on leave from Cracow University of Technology, Warszawska 24, PL-31-155 Cracow, Poland

The paper presents the *Boundary Element Method* (BEM)-based procedure employed for solving inverse thermoelasticity problems. The BEM formulation is used for highly accurate and numerically efficient calculation of sensitivity coefficients. The sets of sensitivity equations are solved with an algorithm in which regularization is inherent via covariance matrices *a priori* and/or *Levenberg-Marquardt* procedure, both combined with function specification approach. The outlined procedure allows one to retrieve the multidimensional boundary condition (BC) distribution in steady-state and transient problems. Strain components and temperatures are used as input data subject to uncertainties. In presented numerical examples the method is capable of reconstructing distributed mechanical and thermal loads with reasonable accuracy.

**Keywords:** thermoelasticity, inverse problems, BEM, sensitivity equations

## 1. Introduction

The need of dealing with inverse problems is, in many areas of research and engineering, of growing and vital importance. Inverse thermoelasticity problems usually seek to determine the unknown thermal and structural boundary conditions. In this class of problems measurement data may contain the measured values of temperatures, fluxes, displacements, and strains. These measurements can be obtained via infrared camera, thermocouples, radar, strain gauges or other measuring devices. In almost all industrial applications the data set includes the measured temperatures (by means of thermocouples) and strain components (using strain gauges). Naturally, all measured quantities are subject to *unavoidable* measurement errors/uncertainties.

In this study we discuss an application of BEM-based technique employed for solving the inverse thermoelasticity problems. The BEM is used for accurate and numerically effective calculation of sensitivity coefficients. The set of sensitivity equations is solved with derived algorithm in which regularization is inherent via covariance matrices *a priori* and/or *Levenberg-Marquardt* procedure, both combined with function specification methodology. The outlined approach allows one to retrieve the multidimensional boundary condition (BC) distribution in steady-state and transient problems.

The accuracy and stability of the algorithms are verified by considering the problems of inverse thermoelasticity with simulated input data specified in the form of strain components and temperatures subject to random errors. In presented numerical examples the method is capable of

reconstructing both mechanical and thermal loads with reasonable accuracy.

## 2. Problem formulation

The governing equations of thermoelastic deformation within an arbitrary domain,  $\Omega$ , enclosed by boundary,  $\Gamma$ , are given by:

$$\rho c \dot{\Theta} = \nabla(k \nabla \Theta) + \dot{q}, \quad (1)$$

$$\nabla^2 \mathbf{u} + \frac{1}{1-2\nu} \nabla(\nabla \mathbf{u}) - \frac{\rho}{G} \ddot{\mathbf{u}} = \frac{2(1+\nu)}{1-2\nu} \alpha \nabla(\Theta - \Theta_{ref}) \quad (2)$$

where  $\rho$ ,  $c$ ,  $k$ ,  $\Theta$ ,  $\dot{q}$ , denote mass density, specific heat, conductivity, temperature, and volumetric heat generation, while  $\nu$ ,  $G$ ,  $\alpha$ ,  $\Theta_{ref}$ ,  $\mathbf{u}$ , Poisson's ratio, shear modulus, coefficient of thermal expansion, reference (*stress-free*) temperature, and displacement, respectively (for plane stress problems equation (2) requires an adjustment of Lamé constants). In thermoelastic deformation analysis structural dynamic effects are usually not of concern and can be neglected.

In inverse analysis the set of boundary condition is specified incompletely, namely, at some portions of the boundary the mechanical and/or thermal load is unknown. Instead, at some points at the external boundary, there is known an information about the process under consideration specified in the form of measured, selected strain components and/or temperatures subject to uncertainties.

Strain and temperature histories at discrete times are given by:

$$\varepsilon(\mathbf{x}_m, t_j) = \bar{\varepsilon}_{m,j} \quad j = 1, 2, \dots, \tau_s, \quad m = 1, 2, \dots, M_s \times n \quad (3)$$

$$\Theta(\mathbf{x}_m, t_j) = \bar{\Theta}_{m,j} \quad j = 1, 2, \dots, \tau_\Theta, \quad m = 1, 2, \dots, M_\Theta \quad (4)$$

where  $\mathbf{x}_m, t_j$  are the location of measuring point and the measurement time, respectively. Subscripts  $s$  and  $\Theta$  stand for strain and temperature, while  $n$  is the number of actually measured strain components.

A frequent situation is, in industrial application especially, that a very limited number of measurement points is available, typically due to geometrical inaccessibility, exposure to severe environment conditions, and most of all, financial cost of obtaining measurement data.

One of possible approaches to reconstruction of multidimensional boundary conditions with the limited number of measurements, is to parameterize their spatial distribution [1], [2], and thus, considerably decrease number of estimated unknowns. Decomposing the total load into its known (superscript  $k$ ) and unknown (superscript  $u$ ) parts, and then approximating the unknown component, yields:

$$\{\mathbf{Q}\}_i = \{\mathbf{Q}\}_i^k + \{\mathbf{Q}\}_i^u = \{\mathbf{Q}\}_i^k + \sum_j a_{ij}^Q \mathbf{Y}_i^Q(\mathbf{x}, \zeta) \quad (5)$$

$$\{\mathbf{L}\}_i = \{\mathbf{L}\}_i^k + \{\mathbf{L}\}_i^u = \{\mathbf{L}\}_i^k + \sum_j a_{ij}^L \mathbf{Y}_i^L(\mathbf{x}, \zeta) \quad (6)$$

where  $\{\mathbf{Q}\}_i$  and  $\{\mathbf{L}\}_i$  represent the thermal and structural loads, respectively, and  $\mathbf{Y}_i$  are spatial functions with knot points,  $\zeta$ , and local coordinates,  $\mathbf{x}$ , whilst  $a_{ij}$  denote unknown approximation parameters at successive time steps,  $i$ . Constitutive strain-displacement relations and some manipulations lead to the set of sensitivity equations in the form of:

$$\{\bar{\Theta}\}_i = [\mathbf{J}]_i^Q \{\mathbf{a}\}_i^Q + \{\mathbf{f}\}_i^Q = [\mathbf{J}]_i^Q \{\mathbf{a}\}_i^Q + \{\mathbf{q}\}_i^k \quad (7)$$

$$\{\bar{\varepsilon}\}_i = [\mathbf{J}]_i^L \{\mathbf{a}\}_i^L + \{\mathbf{f}\}_i^L = [\mathbf{J}]_i^L \{\mathbf{a}\}_i^L + \{\boldsymbol{\varepsilon}\}_i^k \quad (8)$$

where  $[\mathbf{J}]_i$  are Jacobian matrices,  $\{\mathbf{f}\}_i$  free terms vectors, arising from known part of BC(s) set. Vector  $\{\boldsymbol{\varepsilon}\}_i^k$  contains strain components due to thermal expansion,  $\{\boldsymbol{\varepsilon}\}_i^{\text{them}}$ , and prescribed structural loads, and thus, naturally, thermal inverse problem is solved first, followed by inverse elasticity one. In all equations superscripts  $Q$  and  $L$  refer to *thermal* and *structural* parts, respectively.

As the sought-for approximating parameters/variables are those at the boundary, we employ the *Boundary Element Method* (BEM) time-stepping formulation for calculation of entries to the sensitivity coefficients matrices. For completeness in the next Section we outline the procedure and discuss its numerical implementation.

### 3. Sensitivity equations

In this study, we employ the BEM formulation in which the domain integrals appearing in boundary integral representations of both (1) and (2) were converted to boundary-only by means of the *Dual Reciprocity Method* (DRM) [3], exploiting compactly supported *Radial Basis Functions* (RBF). Neglecting inertial and damping structural effects, the resulting set of equations can be written for thermal part as [4]:

$$[\mathbf{H}]\{\Theta\} - [\mathbf{G}]\{\mathbf{q}\} = [[\mathbf{H}][\hat{\Theta}] - [\mathbf{G}][\hat{\mathbf{q}}]]\{\mathbf{b}\} \quad (9)$$

where:

$$\{\mathbf{b}\} = [\mathbf{R}]\{\Theta\} - [\mathbf{F}]^{-1}\{\Theta\}_u \quad (10)$$

and

$$[\mathbf{R}] = [\mathbf{F}]^{-1} \left\langle \sum_{i=1}^1 \text{diag}\{\mathbf{K}\}_i, [\mathbf{F}]_x \right\rangle [\mathbf{F}]^{-1} - \text{diag}\{\mathbf{K}\}_c \quad (11)$$

whilst for elastic deformation as [5]:

$$[\mathbf{H}]\{\mathbf{u}\} - [\mathbf{G}]\{\mathbf{t}\} = [[\mathbf{H}][\hat{\mathbf{u}}] - [\mathbf{G}][\hat{\mathbf{t}}]]\{\mathbf{b}\} + [\mathbf{G}]\{\Psi\} \quad (12)$$

where:

$$\{\mathbf{b}\} = \text{diag}\{\boldsymbol{\alpha}\} [\mathbf{F}]_x, [\mathbf{F}]^{-1}\{\Theta\} \quad (13)$$

$$\{\Psi\} = \bar{\mathbf{D}} \Phi \mathbf{n}; \quad \Phi = \int_{\sigma_n} \alpha \, d\sigma \quad (14)$$

In the foregoing equations  $[\mathbf{H}]$ ,  $[\mathbf{G}]$ ,  $[\hat{\Theta}]$ ,  $[\hat{\mathbf{u}}]$ ,  $[\hat{\mathbf{q}}]$ ,  $[\hat{\mathbf{t}}]$  are coefficient matrices, matrices of particular solutions and their derivatives. Matrices and  $[\mathbf{K}]_b$ ,  $[\mathbf{K}]_c$  contain the reduced derivatives of thermal conductivity, system heat capacity, while matrices  $[\mathbf{F}]$ ,  $[\mathbf{F}]_x$  the RBF interpolation function values, and their derivatives, respectively. Symbols  $\mathbf{D}$ ,  $\boldsymbol{\alpha}$ , and  $\mathbf{n}$  stand for (reduced by modulus of elasticity) coefficient of linear expansion, nodal values of the coefficient of thermal expansion, and unit outward normal vector, respectively.

System of equations (9)–(14) contains many symmetric/anti-symmetric (arising from RBF interpolation) and diagonal matrices, what can be readily exploited while solving and coding, providing meshless treatment of domain integrals, and numerically efficient solution of thermoelastic deformation problem.

Sensitivity coefficient is a measure of the influence of the measured quantity on the shape of retrieved function. The larger value of the coefficient the easier solution of the problem under consideration. If the sensitivity of measurement is small the data coming from this sensor is usually meaningless, decreases accuracy and, moreover, introduces the numerical instability to calculation results due to unavoidable measurement errors [1]. In systems with damping/capacity terms the information of changes in retrieved function *reaches* the measuring point with a delay, depending on the thermophysical properties, geometry, location of the measuring device and/or other factors. Hence, in that type of systems, the temporal distribution has

its maximum several time steps later than that at which measurement was actually taken. This feature is presented in Fig. 1 and 2, where temporal distributions of sensitivity coefficients are given for the cases of retrieving the boundary heat flux (Fig. 1) and temperature (Fig. 2). The influence of the sensor location is also shown, by comparing values of coefficients for measurements taken at the surface at which load is unknown/estimated (internal surface) and at the opposite one (external surface).

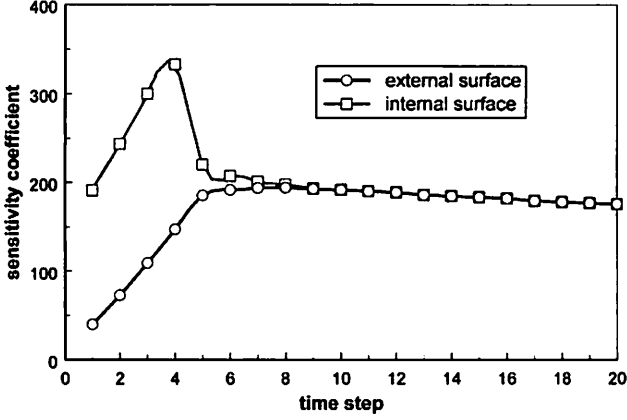


Fig. 1. Example of sensitivity coefficients temporal distribution (heat flux reconstruction)

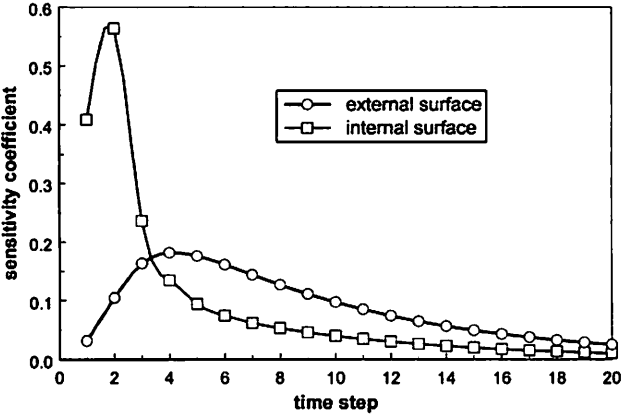


Fig. 2. Example of sensitivity coefficients temporal distribution (temperature reconstruction)

Fig. 1 and 2 demonstrate, furthermore, why exploiting the information from several time steps positively influences the stability and accuracy of solution procedures.

In order to obtain all of entries to sensitivity matrices in equations (7) and (8), at most two multi-load type forward solutions are required, only, [1], [6] providing that measurement time (sampling rate) is constant, what is usually the case. In this work the outlined BEM-DRM formulation is employed for that purpose, resulting in highly accurate calculation of sensitivity coefficients. In the following Section the technique used for solving that system is discussed.

#### 4. Estimation of load approximating parameters

Stability of computational procedures, in dealing with transient problem, can be significantly increased by exploiting the *Function Specification* method. The standard approach assumes that function representing the temporal distribution is piece-wise constant. This allows one to easily solve the set of sensitivity equations as the coefficients are not inter-dependent in time (*coupled in time*) and simple sequential methods can be implemented. The main disadvantage of such procedure is, usually, fast accumulation of errors, as the estimated parameters from previous time steps enter the free terms vector of the subsequent one. It may result in the substantial decrease in quality of estimation, at the final steps of the process, especially.

Two techniques are implemented here to increase the accuracy of the boundary conditions/loads reconstruction, namely, piece-wise linear approximation of temporal load distribution and, the procedure, which allows us to take into consideration an arbitrary number of data sets/time steps. This procedure is briefly discussed below.

The set of sensitivity equations is restated in the form of *constraints equations*, namely:

$$[\hat{\mathbf{J}}]_i \{\varphi\}_i = \{\hat{\mathbf{f}}\}_i \quad (15)$$

$$[\hat{\mathbf{J}}]_i = [-\mathbf{I}_i, \mathbf{J}_{i,1}, \dots, \mathbf{J}_{i,J}] = [-\mathbf{I}_i, \bar{\mathbf{J}}_i] \quad (16)$$

where  $[\hat{\mathbf{J}}]_i$ ,  $\{\varphi\}_i$ , and  $\{\hat{\mathbf{f}}\}_i$ , denoting the Jacobian matrix, estimated variables and residual vectors while subscripts  $i, j, J$  stand for considered time, measuring time, and number of measurement sets taken into analysis, respectively. Vectors of estimated variables contain also unknown BC values, namely, their approximation parameters:

$$\{\varphi^{\varrho}\}_i^T = \{\bar{\Theta}_i, \mathbf{a}^{\varrho}\}_i \quad (17)$$

$$\{\varphi^L}\}_i^T = \{\bar{\epsilon}_i, \mathbf{a}^L}\}_i \quad (18)$$

The estimates of load interpolation parameters can be sequentially obtained from:

$$\{\mathbf{a}\}_{i,j} = \{\mathbf{a}\}_{i-1,j} + \{\mathbf{v}\}_{i,j} \quad (19)$$

$$\{\mathbf{v}\}_{i,j} = \{\mathbf{v}\}_{i-1,j} + [\mathbf{P}]_i [\mathbf{D}]_i^{-1} \{ \{\hat{\mathbf{f}}\}_i - [\bar{\mathbf{J}}]_i \{\mathbf{v}\}_{i-1,j} \} \quad (20)$$

with auxiliary matrices defined as:

$$[\mathbf{D}]_i = [\bar{\mathbf{J}}]_i [\mathbf{P}]_i + [\mathbf{W}]_i \quad (21)$$

$$[\mathbf{P}]_i = [\mathbf{C}]_{i-1} [\bar{\mathbf{J}}]_i^T \quad (22)$$

$$[\mathbf{C}]_i = [\mathbf{C}]_{i-1} - [\mathbf{P}]_i [\mathbf{D}]_i [\mathbf{P}]_i^T \quad (23)$$

and where  $[\mathbf{W}]_i$  is diagonal weighting matrix,  $\{\mathbf{v}\}_{i,j}$  are correction to preliminary estimates of load approximation

parameters, while set-up values of  $[C]_{j=0}$  equal to their assumed/calculated *covariances a priori*. The algorithm is exploiting and including in the procedure measurement data from successive time steps, updating the previously calculated estimates. As the algorithm takes into account the covariances of previous sub-solutions, additional regularization is achieved.

This approach allows one to take into account an arbitrary number of time intervals/steps,  $J$ , for estimation of load approximating parameters, however, it should be pointed out that as inter-dependency between measured data and estimated parameters separated by large time interval may be weak, it is usually practical to include only a few (3 to 4) steps.

## 5. Numerical examples

This Section includes two numerical examples illustrating capabilities of the technique, demonstrating its robustness and stability. The first example deals with the transient thermoelastic deformation while the second presents the reconstruction of time-invariant loads in the case involving functionally graded material.

### 5.1. Inverse transient thermoelasticity problem

Let us consider the 2D inverse thermoelasticity problem in domain subjected to plane strain loading conditions. The geometry and dimensions of the domain are given in Fig. 3.

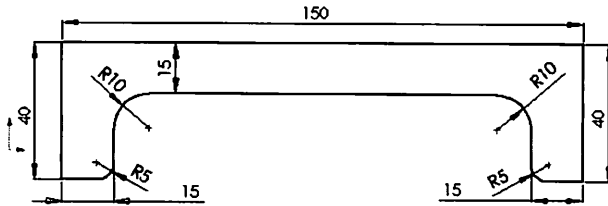


Fig. 3. Domain geometry and dimensions

Thermophysical properties of the domain material were assumed constant and that of the typical stainless steel, namely,  $E = 210$  GPa,  $\nu = 0.33$ ,  $\alpha = 1.2 \text{ E-}5$  1/K,  $\rho = 7820$  kg/m<sup>3</sup>,  $k = 47.4$  W/mK,  $c = 473.4$  J/kgK.

As known external thermal BC(s) the following values of heat transfer coefficients and ambient temperatures were applied:  $h_1 = 1100$  W/m<sup>2</sup>K,  $T_{\Omega_1} = 10^\circ\text{C}$ ,  $h_2 = 900$  W/m<sup>2</sup>K (convective BC (1) – Fig. 4) and  $T_{\Omega_2} = 5^\circ\text{C}$  (convective BC(2) – Fig. 4). The external surface was considered as thermally insulated and, in structural analysis, left and right edges as fully restrained. Both the thermal (heat flux) and mechanical loads (pressure) at *top* face were *unknown*.

The location of measurement points is given in Fig. 4, where  $s$  and  $T$  stand for strain and temperature, respectively. In the example under consideration temperatures were known/measured at 3 points (1T–3T). All measurements were subject to random errors of amplitudes as high as  $0.5^\circ\text{C}$  for temperatures and  $8.0 \text{ E-}06$  for strain components (two components measured). It was assumed, furthermore, that the measurements were taken every 2 s.

Sensitivity coefficients were obtained using BEM time-stepping DRM formulation (equations (9)–(14)). In order to

achieve the higher accuracy, the quadratic approximation in time was employed (except for the very first time step when linear approximation is used) [4].

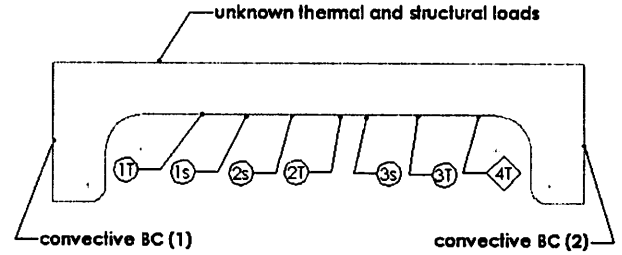


Fig. 4. BC(s) and measurement points location

The geometry was discretized with 62 quadratic boundary elements and 66 points in the domain. The BEM mesh and location of internal points is given in Fig. 5.

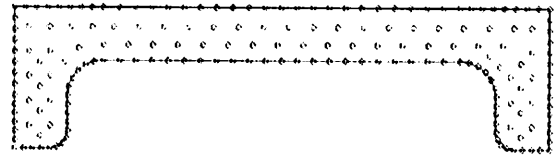


Fig. 5. Mesh and internal points locations

It is worth emphasizing, that the data and error levels, along with the location of measurement points, were selected to be the most unsuitable for any method of inverse analysis, and served here as a good test, verifying both robustness and stability of the presented approach. The *piece-wise linear* temporal distribution approximation was used with  $J = 3$  (3 time-steps *filter length*).

In Figures 6, 7, and 8 selected calculation results are presented. Fig. 6 shows the estimated and exact heat flux distributions and 50 and 180 s, Fig. 7 presents recovered pressure distribution at time  $t = 180$  s, while Fig. 8 gives the domain temperature plot at time  $t = 200$  s.

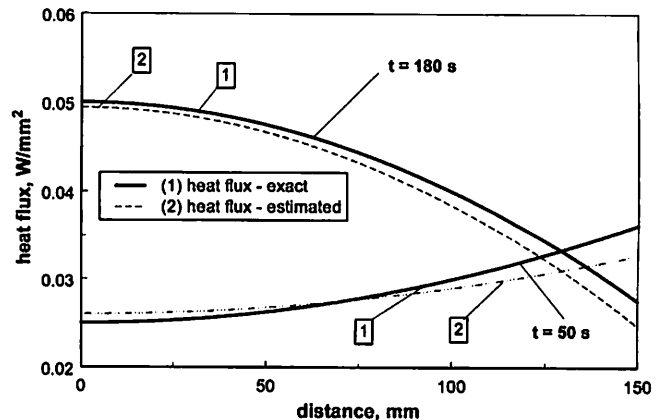


Fig. 6. Retrieved distribution of boundary heat flux

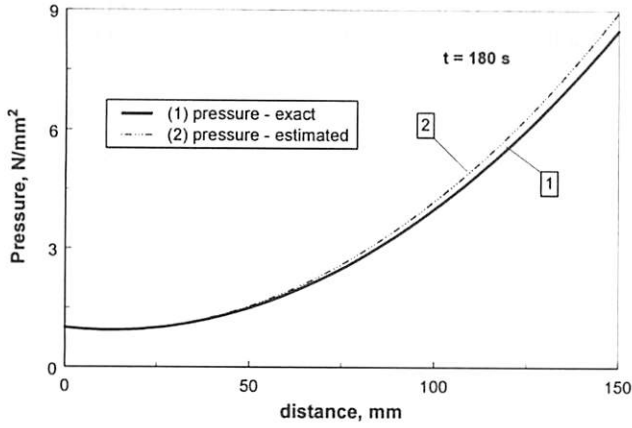


Fig. 7. Retrieved spatial pressure distribution

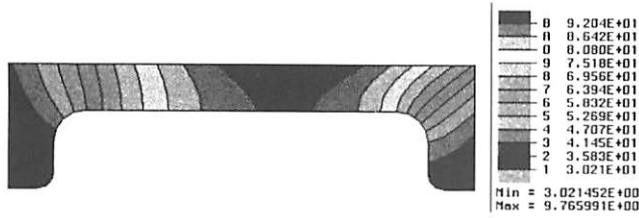


Fig. 8. Temperature distribution at time  $t = 200$  s

Despite that the number of measurements used was very limited, non-linear load distribution applied and, furthermore, the measurements taken at the opposite boundary, the algorithm was still capable of reconstructing both the spatial and temporal load distribution with reasonable accuracy.

## 5.2. Inverse problem with functionally graded material

In this example the steady-state analysis of thermoelastic deformation is presented. The geometry of the problem and dimensions are kept that of the previous sub-section. The thermal conductivity of the material was assumed to be given as:

$$k = 52 + 150x_1 + 100x_2 \quad [\text{W/m}\cdot\text{K}] \quad (24)$$

Remaining boundary conditions and material properties are those of Example 1. As unknown boundary condition at the top surface of the domain the non-linear temperature (thermal restraints) and pressure (structural load) were assumed.

The measured temperatures were given, again, at 3 points (1T–3T) and, additionally, at point 4T (Fig. 4). Strain components were specified at points 1s–3s (Fig. 4). In this example the unknown load approximating parameters were estimated using an iterative *Levenberg-Marquardt* technique [7]:

$$\{\mathbf{a}\}^{k+1} = \{\mathbf{a}\}^k + [\mathbf{J}]^T [\mathbf{J}] + \mu^k [\mathbf{I}]^{-1} [\mathbf{J}]^T \{\mathbf{r}\}^k \quad (25)$$

where  $k$  stands for the number of iteration,  $\mu$  is a damping parameter calculated using scaled trust-region approach, and  $\{\mathbf{r}\}$ , again, denotes the residual vector. The numerical results were obtained using the subroutine given in [8] with default settings/values of all parameters.

Different levels of measurement noise were considered. Fig. 9 presents retrieved space-variation of boundary temperature (symbol T) and pressure (symbol P) for errors as high as  $0.3^\circ\text{C}$  for measured temperatures and  $6.0 \text{E}-06$  for strain components, whilst Fig. 10 and 11 show the retrieved domain temperatures and deformed shape of the domain, respectively.

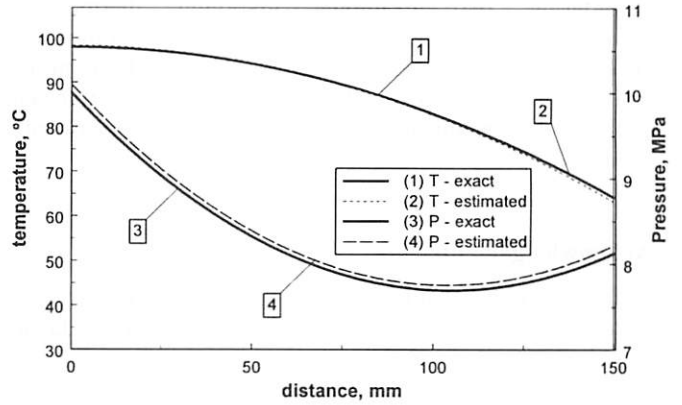


Fig. 9. Reconstructed load spatial distribution

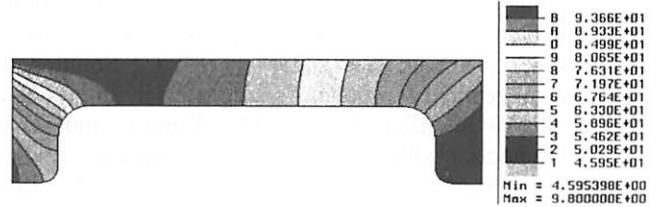


Fig. 10. Reconstructed temperature distribution



Fig. 11. Deformation (displacements magnitude)

## Conclusions

In this study we presented an application of the DRM time-stepping BEM formulation to highly accurate calculation of sensitivity coefficients in transient and steady-state thermoelasticity. The formulation contains many symmetric/anti-symmetric matrices, what can be readily exploited while solving and coding. Furthermore,

unknowns, which appear in the BEM analysis, are precisely the variables of interest in inverse reconstruction of mechanical and/or thermal loads, leading to substantial savings in resources and time (as intricate, high quality domain meshes are not required). The system of sensitivity equations in time-dependent case was solved by means of the procedure with *a priori* covariance matrices while the *Levenberg-Marquardt* method was employed in the steady-state one. In transient case, the implemented procedure reduces the accumulation of errors both by the highly accurate calculation of sensitivity coefficients and a special approach in handling the minimization problem.

In the paper, reconstruction of heat flux, temperature and pressure distribution is demonstrated. The stability, efficiency and accuracy of the algorithm were verified considering two examples involving thermoelastic deformations. As measurements selected strain components and temperatures were used. In presented numerical examples, method is capable of reconstructing transient, distributed mechanical and thermal loads with reasonable accuracy.

#### Acknowledgements

Authors gratefully acknowledge support of *Japan Society for the Promotion of Science* and Shinshu University, Japan.

#### References

1. Bialecki, R.A., Divo, E., Kassab, A.J., Ait Maalem Lahcen, R., Explicit calculation of smoothed sensitivity coefficients for linear problems, *Int. J. Numer. Meth. Engng*, John Wiley & Sons, **57**, pp. 143 –167, (2003).
2. Nowak I., Nowak A.J. and Wrobel L.C., Solution of inverse geometry problems using Bezier splines and sensitivity coefficients. In M. Tanaka and G.S. Dulikravich, editors, *International Symposium on Inverse Problems in Engineering Mechanics III, ISIP 2001*, Nagano, Japan, Elsevier Science, pp. 87 – 95, (2001).
3. Partridge, P.W., Brebbia, C.A., Wrobel, L.C., *The Dual Reciprocity Boundary Element Method*, Computational Mechanics Publications, (1992).
4. Tanaka, Masa., Matsumoto, M., Takakuwa, S., DRM applied to the time-stepping BEM for transient heat conduction, R. Gallego, M. H. Aliabadi (editors), *4<sup>th</sup> International Conference on Boundary Element Techniques (BeTeQ)*, July 15-17, 2003, Granada, Spain, pp. 79-84, (2003).
5. Okayama, S., Matsumoto, T., Tanaka, Masa., A study on thermoelastic analysis using dual reciprocity boundary integral formulation (in Japanese), *Transactions of JASCOME*, **17**, pp. 7–10, (2000).
6. Tanaka, Masa., Guzik, A., Bialecki, R., Matsumoto, T., *Reconstruction of multidimensional boundary condition distribution in elasticity problems using FEM-based filtering technique*, *Transactions of JASCOME*, **3**, pp. 33-38, (2003).
7. Dennis, J. E., Schnabel, R. B., *Numerical Methods for Unconstrained Optimization and Nonlinear Equations*, SIAM, Philadelphia, (1996).

8. Press, W. H., Teukolsky, S. A., Vetterling, W. T., Flannery, B. P., *Numerical recipes in Fortran 90*, **2**, Cambridge University Press, 2<sup>nd</sup> Edition (1996).